5-12-2020

Spectral Observations of the 2019 South American Total Solar Eclipse

Sarah Auriemma
Bridgewater State University

Spectral Observations of the 2019 South American Total Solar Eclipse

Sarah Auriemma

Submitted in Partial Completion of the
Requirements for Departmental Honors in Physics

Bridgewater State University

May 12, 2020

Dr. Martina Arndt, Thesis Advisor
Dr. Jeff Williams, Committee Member

BRIDGEWATER STATE UNIVERSITY | PHYSICS DEPARTMENT

Spectral Observations of the 2019 South American Total Solar Eclipse

Sarah Auriemma

May 12, 2020

Abstract

On July 2, 2019, a total solar eclipse was visible in parts of Chile and Argentina. I joined the Solar Wind Sherpas, an international group of scientists, engineers, students, and eclipse enthusiasts, to South America to make observations of the solar corona (the Sun's upper atmosphere) during the eclipse. The Sherpas were split into three teams along the path of totality and my group was stationed at Mamalluca Observatory in Vicuna, Chile. One of the instruments we used at this side was a three-channel (red, green, and blue) spectrometer designed by A. Ding, of Hawai'i's Institute for Astronomy. Spectra from the corona can be used to study coronal composition and ion speeds. I helped assemble and align the spectrometer in Chile and performed preliminary analysis of spectral data taken at our site.

CONTENTS

1 Acknowledgments **4**

2 Introduction **5**

2.1 The Sun 5

2.2 Spectroscopy 12

3 Methods **14**

3.1 Pre Eclipse Data Collection 14

3.2 Location of 2 July 2019 Total Solar Eclipse 16

3.3 Equipment 18

3.4 Spectrograph 19

4 Data **23**

4.1 Data Collection 23

4.2 Data Analysis 24

4.3 Hydrogen 26

4.4 Helium 27

5 Conclusion and Future Work **28**

1 ACKNOWLEDGMENTS

Thank you to Dr. Shadia Habbal, the lead Solar Wind Sherpa, for making it possible for me to experience research in the field. All the instruments and experiments were designed at the Institute for Astronomy (IfA) and Dr. Habbal coordinated the vast number of details required for an expedition like this. Thank you to the staff at the IfA for all their administrative support as well. Dr. Ding designed the spectrometer I helped assemble - special thanks to B. Boe who taught me so much about how the spectrometer works, and Bryan Yamashiro for helping me understand how to begin to analyze spectrometer data at a graduate level. Thank you to Dr. Arndt for being my patient mentor and giving me the invaluable lesson that science always comes first. I would like to thank the entirety of the Physics department at BSU- faculty, staff, and students - for all their support and friendship. Special thank you to J. Kern for her guidance with Maxim DL over the years. Thank you to the team at Cyanogen for granting me with a temporary Maxim DL Pro license to help finish the image processing necessary for completing this thesis during the unfortunately named *corona* virus pandemic. Funding for this project was provided by NSF RAPID grant to the Institute for Astronomy: *AGS*1834662, NASA Space Grant, Massachusetts Space Grant consortium, and the Adrian Tinsley program at Bridgewater State.

2 INTRODUCTION

2.1 THE SUN

The Sun is our closest star, located at the center of the solar system. The Sun provides a source of energy and light for our planet. By studying the Sun (particularly during a total solar eclipse), we can start to understand how it works and how the Sun influences our Earth.

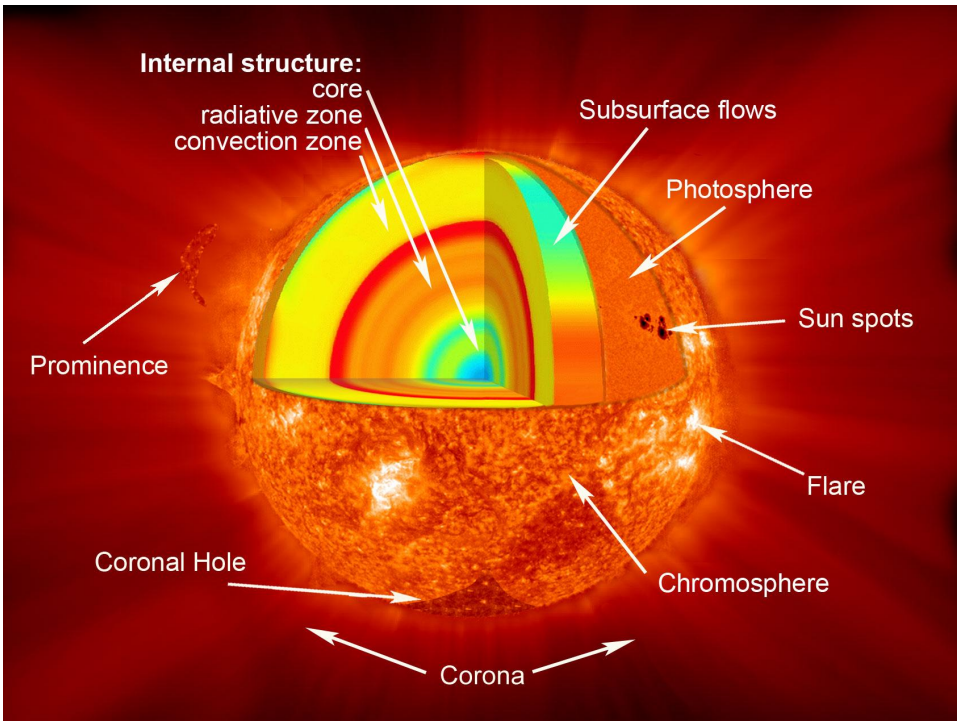

Figure 2.1: Layers of the Sun. [5]

The Sun is not a solid mass, but a hot ball of plasma. Sitting $1.496x10^8 km$ ($1 Au$, or astronomical unit) away from Earth, its gravitational field pulls planets around it. The Sun has its own rotation as well; the plasma on the Sun does not rotate in a uniform velocity. The plasma at the poles move slower than the equator; it takes about 27 days for the equatorial regions to make one solar rotation, while the polar regions take more than one Earth month.[9] This movement allows the magnetic field to wrap around the Sun and along the

equator. The magnetic fields interact with the plasma and play a role in creating features like sunspots, coronal holes, solar flares, and prominences.

The Sun is made up of different layers (see figure 2.1). At the center is the core. This is the hottest part of the star at a temperature of $1.5x10^7K$ ($2.7x10^{7\circ}F$)[7]. The core is where a majority (99%) of nuclear fusion of the Sun occurs. The Sun is mostly composed of Hydrogen. Nuclear fusion is the process through which stars convert Hydrogen into Helium, which is the majority of the Sun's composition. Next is the radiation zone, in which energy from the core travels outward via radiation instead of thermal convection [5]. The interface layer (not featured in figure 2.2) is where the Sun's magnetic field is theorized to be generated by shifting plasma, which can shift and stretch its magnetic field lines. The convection zone is much cooler than the other solar interior layers. Its temperature of $2x10^6K$ ($3.6x10^{6\circ}F$) is cool enough for heavy ions to hold into their electrons. This process makes the material more opaque so that is is more difficult for radiation to get through [5]. Convective activity happens within the plasma, and currents develop to push the Sun's thermal energy outward.

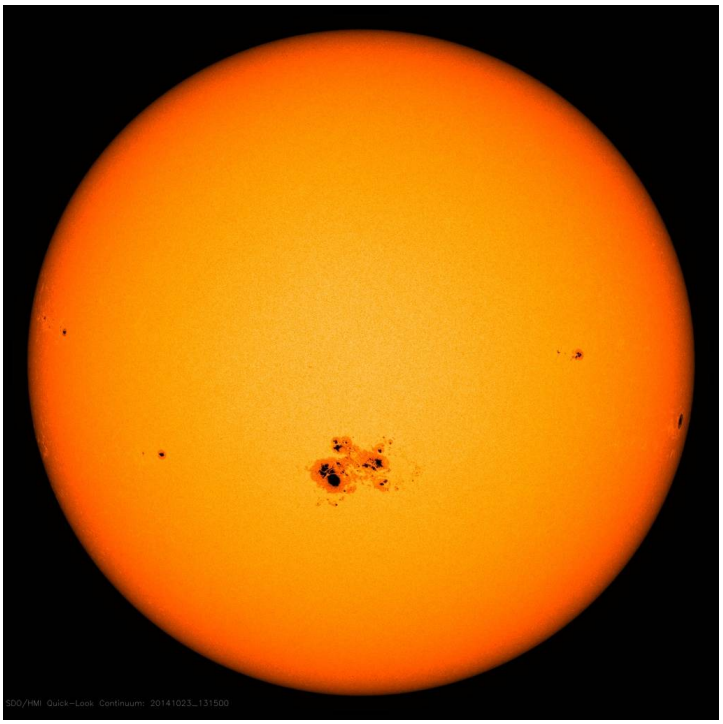

Figure 2.2: The Sun Photo taken from Solar Dynamics Observatory.

The *photosphere* is the visible surface of the Sun, where the light within is radiated outward in all directions. Optical radiation from this surface is what we see with our eyes eight minutes after it leaves the Sun. This layer has a temperature ranging from $4.5x10^3K$ – $6x10^3K$ ($7.6X10^3 - 1X10^4°F$). The photosphere can be observed with telescopes with solar filters (as to not damage the telescope mirrors or the human eye), and sun spots can be seen on the surface. Sun spots appear darker as they are a lower temperature than the rest of the photosphere (typically $3.7X10^3K$ or $6.2X10^3°F$). These spots indicate strong magnetic regions poking out of the solar surface.

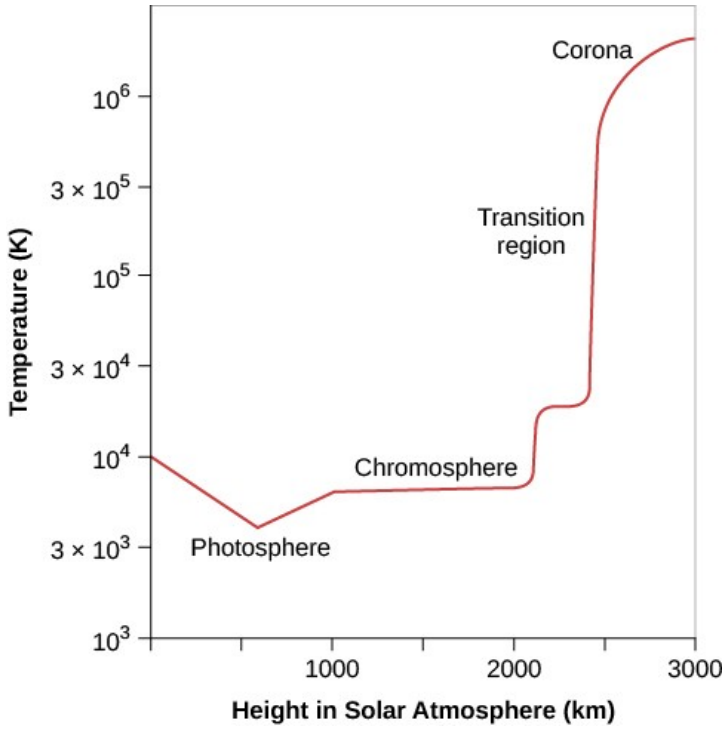

Figure 2.3: Temperatures in the solar atmosphere: On this graph, temperature is shown increasing upward, and height above the photosphere is shown increasing to the right. Note the very rapid increase in temperature over a very short distance in the transition region between the chromosphere and the corona[4].

The layer of the Sun immediately above the photosphere is the *chromosphere*. This layer can be seen during a total solar eclipse (TSE), when the very bright photosphere is blocked by the moon during totality. The chromosphere contains a high density of hot hydrogen, which gives the layer a distinctive red/pink color. The density of this layer is 10^{-4} times that of the photosphere, which makes it invisible to the human eye without special equipment (refer to section 3.3 for more information). The temperature of this layer varies from $3.8X10^3K$ to $3.5X10^4K$ (or $6.3X10^3°F$ to $6.3X10^4F$), increasing with height (see figure 2.3).

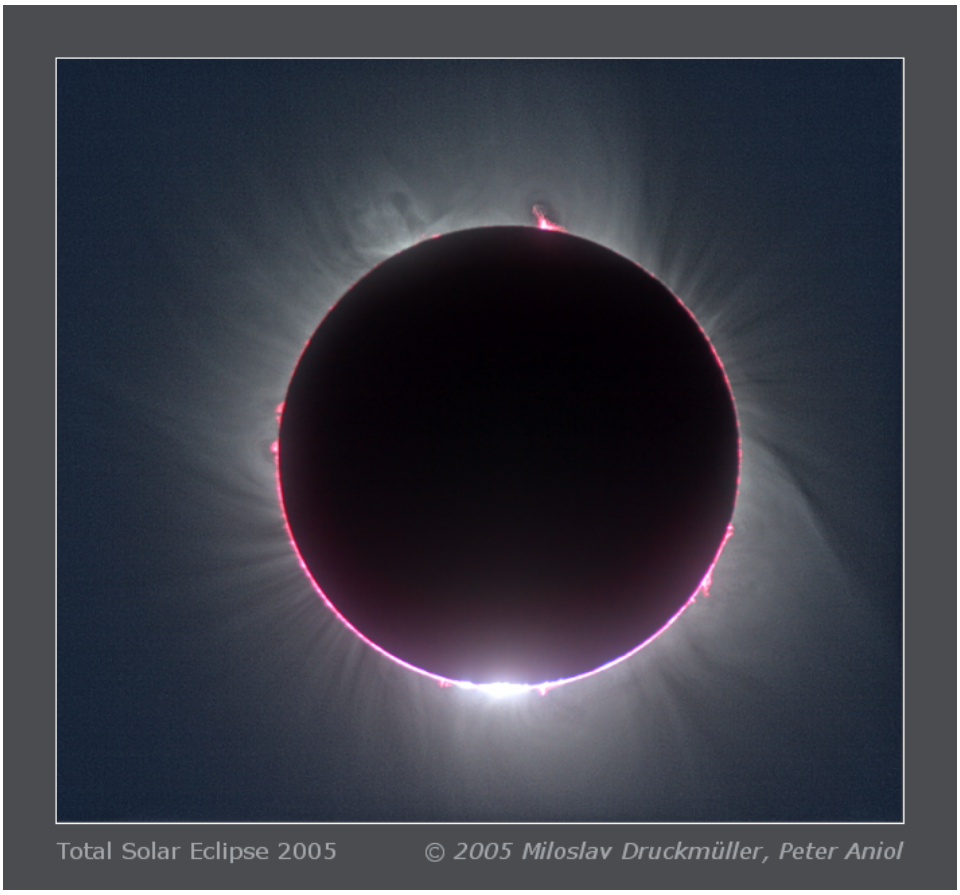

Figure 2.4: The pink chromosphere can be seen during totality of the 2005 total solar eclipse. [8]

Surrounding the chromosphere and the internal layers of the Sun is the faint (but very hot) atmosphere, called the *corona*. The plasma within the corona is on the order of $1x10^6K$ ($1.8X10^6°F$), which is two orders of magnitude hotter than the photosphere. Note that, when stepping away from a heat source (in this example, the Sun's core), we expect to experience a cooler temperature. This is called the *coronal heating problem*, and is an unsolved problem in physics.

The corona has features that stem from *active regions*. *Solar flares* are sudden increases of brightness and energy caused by shifting magnetic activity near sun spots. A *prominence* is a large, bright, gaseous loop that is anchored to the surface of the Sun. Recall that the corona is made up of hot ionized plasma, which does not emit much visible light compared

to the surface of the Sun below. Prominences contain cooler plasma that is more luminous and denser than the plasma of the corona. Prominences have magnetic fields that have the potential to build up and break, which lead to coronal mass ejections (CMEs). *CMEs* are explosions in the corona that eject beyond the Sun's atmosphere and have the potential to impact other planets, affecting magnetic fields, radios, and atmospheres. CMEs and solar flares become more frequent as the *solar cycle* increases to a maximum.

Around every eleven years, the Sun's magnetic poles flip. This cycle is directly related to amount of activity on the surface of the Sun, such as sunspots [7] (see figure 2.5). An increase in number of sunspots is correlative with an increase in magnetic activity. These vary with the solar cycle.

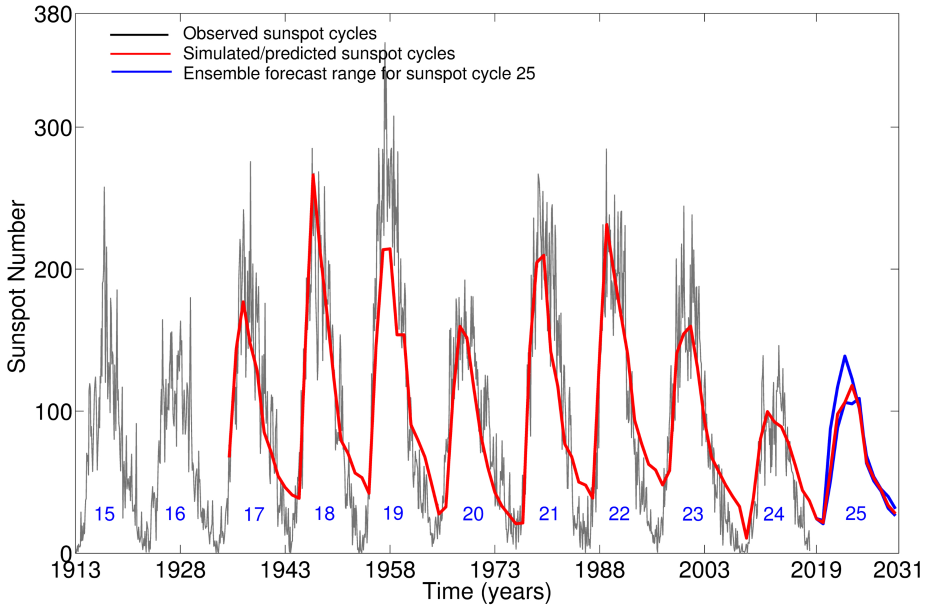

Figure 2.5: Sunspot numbers plotted against predictive data for solar cycles from 1913 to 2031. [2]

During a total solar eclipse, the corona becomes visible due to the moon blocking out the bright photosphere. The visibility of the corona only occurs during a total solar eclipse, not a partial or annular. Because the corona is observable during a total solar eclipse, it is important to take advantage of the short time period of totality (typically lasting a few

minutes).

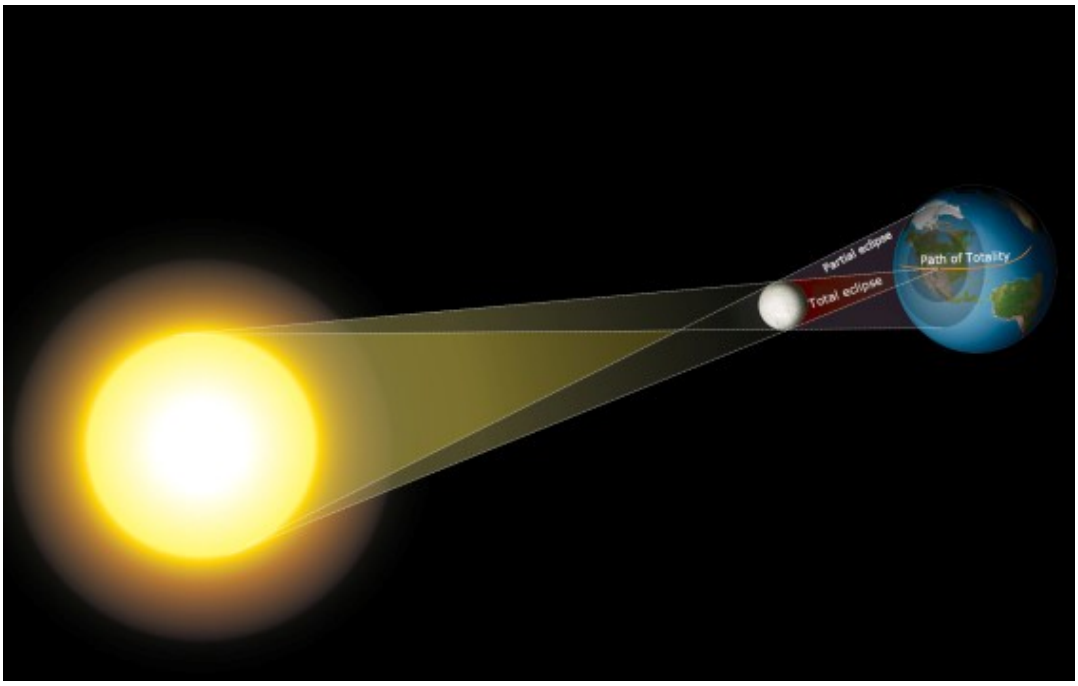

Figure 2.6: Geometry of a total solar eclipse. [1]

It is important to note the geometry and timeline of total solar eclipses (see figure 2.6), so the orientation of the Sun can be deciphered during data analysis. The point at which the moon first crosses over the Sun before totality is known as *first contact*, or C1. *Second contact*, or C2 is the point at which the totality starts. Just before C2, the *diamond ring* and *Baily's beads* effects happen. Irregularities of the Moon's topography causes beads of light from the Sun to shine through the total eclipse. Orientation of the Baily's beads change depending on location of observations and be used in data analysis. Totality ends with *third contact*, or C3 and another diamond ring. *Last contact*, or C4 is the last moment where the moon crosses over the Sun. The path of the Moon's shadow on the Earth is called the *path of totality*. This is where a total solar eclipse can be seen from (see the shadow in figure 2.6).

As seen in figure 2.5, the 2019 TSE occured during a solar minimum, therefore the magnetic activity of the Sun was minimal. Therefore, as expected, the TSE did not have many features to observe as opposed to the TSE in 2017, which was a more active Sun.

2.2 SPECTROSCOPY

Spectroscopy is the study of matter using light. By analyzing spectra of visible light collected via a spectrometer, we can determine things such as the chemical makeup and speed of ions in solar plasma. By using a *spectrograph* to observe the light of the corona, we can better understand the dynamics of the environment above the solar surface.

A spectrograph consists of a diffraction grating, a slit, and a photo-detector (or camera). More advanced designs which involve the use of filters, dichroic mirrors, beam splitters, and converging/diverging lenses. We used an echelle spectrograph, which uses an echelle grating. Echelle gratings have large stair-like spacing, and spectrometers using these gratings can take advantage of the high spectral resolution that occurs at the higher orders of diffraction.

Higher-order spectroscopy is needed in solar eclipse research, since the emission from the Sun produce different spectra that overlap on a low-order diffraction grating. It is necessary to widen the distance between the spectra by upping the order of diffraction. The order of diffraction used in the spectrometer in this project was 42. By knowing the step size between the echelle gratings, and the slit size, one can calculate the order difference.

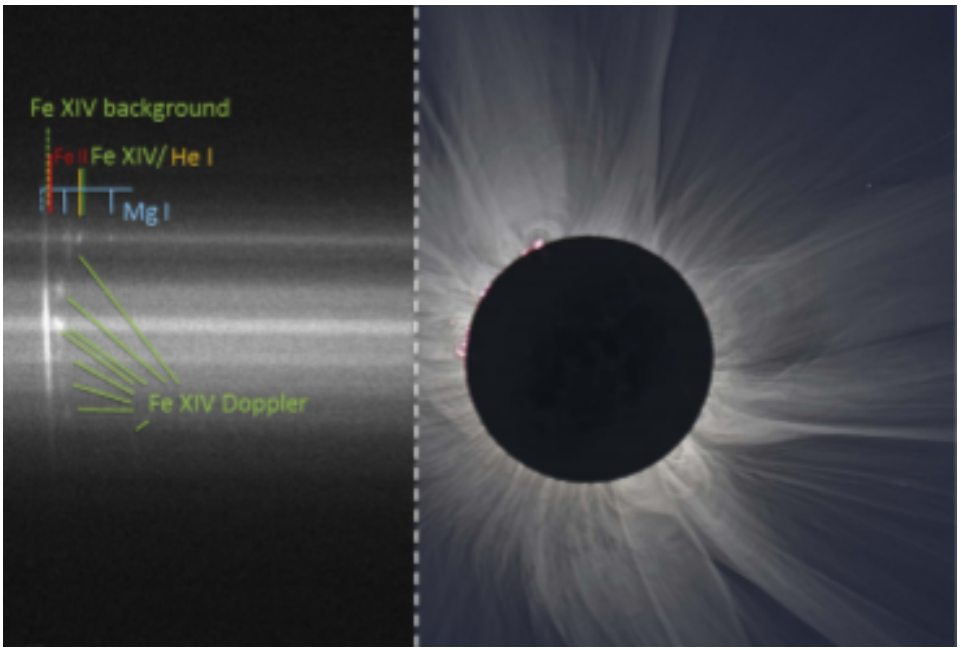

Figure 2.7: Two-dimensional spectra overlaid on a white-light eclipse image to show position in corona. [6]

Figure 2.7 shows a white light image of the 20 March 2015 total solar eclipse. The spectrometer slit was positioned along the dotted line, and the resulting spectrum is shown on the left. Spectral lines from Fe XIV, He I and Mg I are evident. The Fe XIV line is Doppler shifted and when analyzed, showed line of sight speeds of up to $1500 km/s$ [6].

3 METHODS

3.1 PRE ECLIPSE DATA COLLECTION

It is important to monitor the Sun's activity before a total solar eclipse to help predict and prepare for what the corona could look like. In preparation for the 2019 TSE, I wrote a Python script to generate movies from data of the rotating Sun in various wavelengths (see figure 3.1). These data were taken by The Solar Dynamics Observatory (SDO), a satellite launched in 2010 by NASA. SDO's data is published daily, freely available to the public [1].

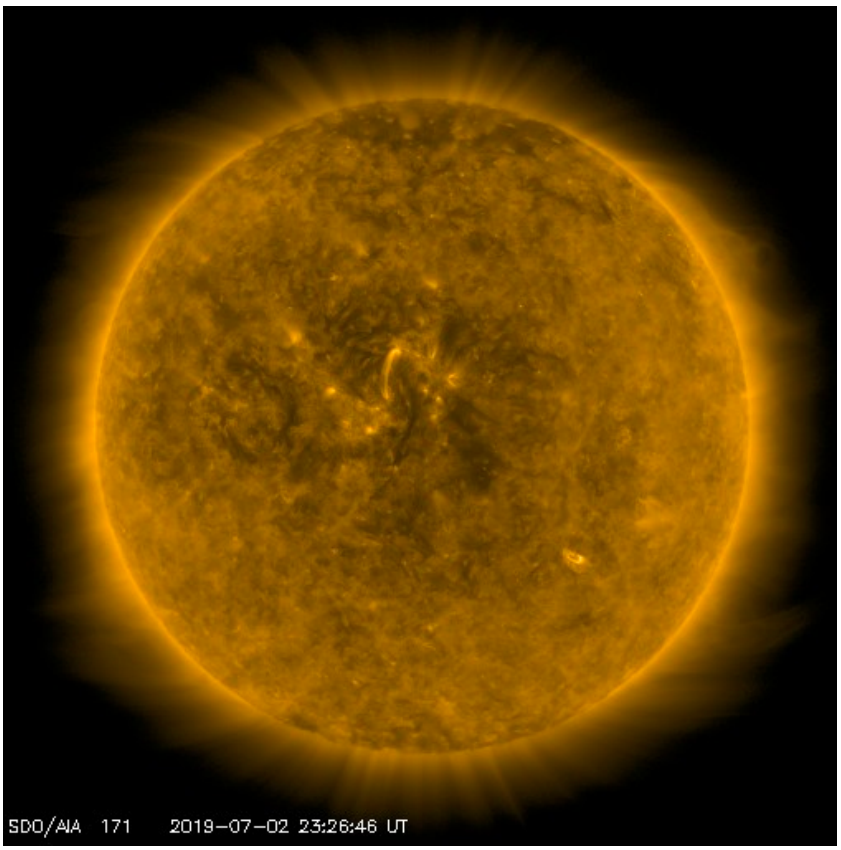

Figure 3.1: Capture from SDO data from day of July 2, 2019 TSE, in wavelength 171$\mathring{A}$.

[1] sdo.gsfc.nasa.gov

I generated movies in various wavelengths: 171$\mathring{A}$, 193$\mathring{A}$, and 6173$\mathring{A}$ using data taken from June 1, 2019 to July 3, 2019 [2].

Although the Sun was approaching minimum activity, features were still present, such as a prominence on the right limb of the Sun. Unfortunately, none of our observing sites captured data from this feature.

[2] https://sites.google.com/student.bridgew.edu/solaractivityauriemma

3.2 Location of 2 July 2019 Total Solar Eclipse

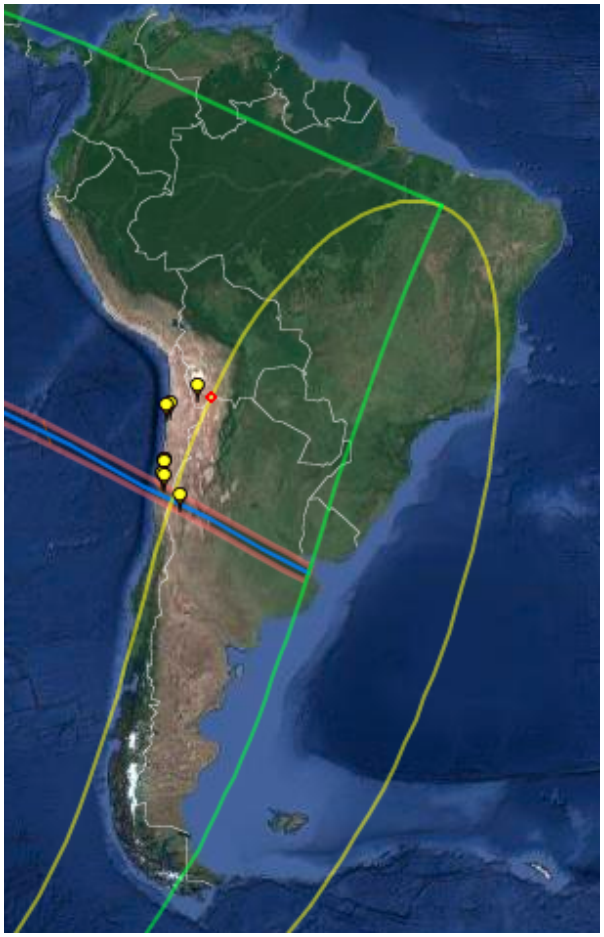

Figure 3.2: The path of totality over South America. Parts of our team observed from both Chile and Argentina.

The width of the band of totality for the 2 July 2019 total solar eclipse was at maximum $161km$ ($100mi$). Totality could be seen in Chile and parts of Argentina (see figure 3.2)[3]. Our 27 person team split into three groups observing across the path in both countries. The observing site for our ten person team was located at the Mamalluca Observatory in Vicuña, Chile (see figure 3.3).

[3]Map taken from `http://xjubier.free.fr`

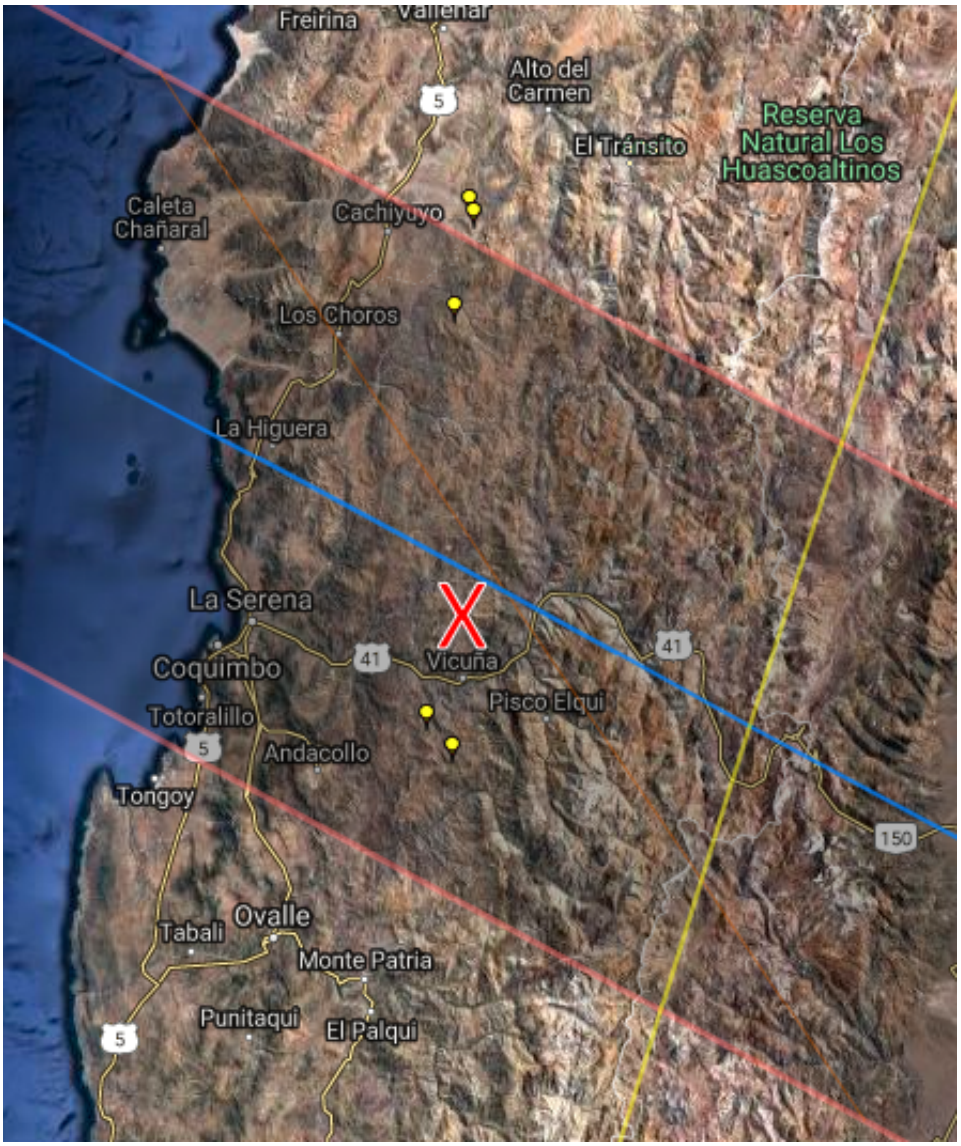

Figure 3.3: Our observing site, Mamalluca Observatory is located on the map indicated by the red x. The coordinates for this site are 29°59′23.8" S and 70°41′07.4" West.

This observatory is normally open for public use, but was only open to scientific observing teams and press for the 2019 South American TSE. This observing site will be further referred to as *Mamalluca*.

3.3 EQUIPMENT

At Mamalluca, the team utilized three different sets of equipment: A white light system, a narrow band imager, and a spectrometer.

The white light system (see figure 3.4) was comprised of multiple telescopic lenses attached to DSLR cameras. This system can be used to study coronal magnetic field structures. To see an image taken by this white light system, see figure 5.1.

Figure 3.4: T. Bedel setting up white light imagers at the 2017 eclipse. Photo by R. Havasy.

The narrow band imager was a system of 6 lenses, CCD cameras, and filters designed to let in specific wavelengths (to observe specific elements). Using this system, we observed ArX (553.4nm), FeXI (789.2nm), and FeXIV (530.3nm).

3.4 SPECTROGRAPH

The spectrometer (figure 3.5) was operated by Insitute for Astronomy graduate student, Ben Boe. The optical equipment within the spectrometer was aligned by Ben Boe with my assistance over the course of two days. I also assisted in mounting the spectrometer to the tripod for observing.

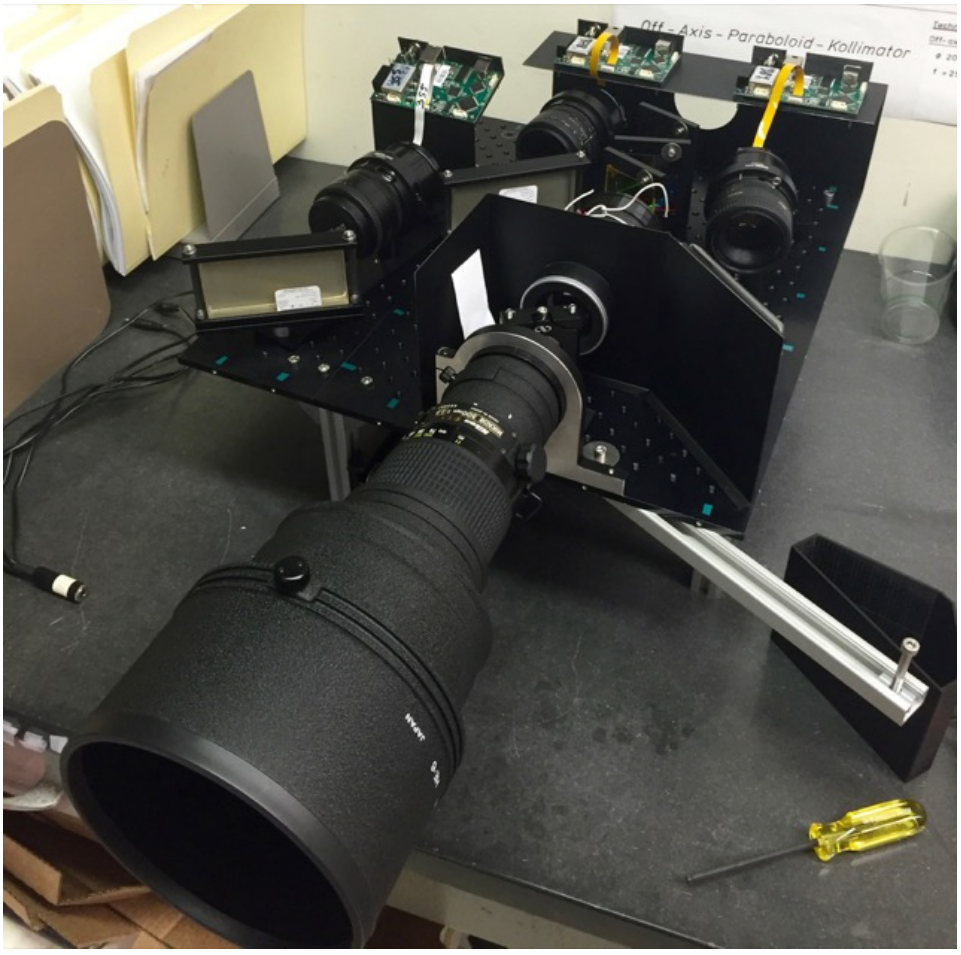

Figure 3.5: View of unmounted spectrograph under construction with the 300mm lens mounted on the front. [3]

A. Ding designed a 3-channel spectrometer for each of the three observation sites. At previous eclipses, a two-channel spectroscopy design was used, but for this eclipse, another channel was added. The new spectrometer (see figure 3.7) has three cameras to record spectra in the red, green, and blue channels. A fourth camera is used to observe the loca-

tion of the slit in the corona throughout the eclipse. The time stamps from all 4 cameras make it possible to correlate the data with respect to time.

A. Ding designed the three channel spectrometer to be portable enough so it could be a carry-on luggage (since this equipment is fragile and cannot be checked or shipped), and to be assembled outside of a laboratory. After arriving in Chile, I assembled the spectrometer with B. Boe (figure 3.6).

The process of assembly took place over two days, and a makeshift dark room was required to ensure no light leaked into the spectrometer while performing calibration in each channel utilizing colored lasers and a spectral lamp. Mamalluca observatory allowed our team to use a planetarium as this dark room. This was particularly helpful; if there had been no indoor dark room, assembly would have to take place outside which could have allowed dust within the optics of the instrument.

Figure 3.6: B. Boe, Ph.D. candidate at Institute for Astronomy (left) and Sarah Auriemma, undergraduate at Bridgewater State University (right) assembling the three-channel spectrometer at the Mamalluca site, 2019.

This assembly required precise alignment of the mirrors and gratings to ensure no light leaks, loss, or interference between the channels.

After assembly and alignment, calibration spectra were taken using of spectral lamps. This calibration was performed in a dark room to ensure no light leaks. Calibration images were taken in all three channels at various exposure times matching the times of the planned light frames of the eclipse. The elements used for calibration were Argon, Water, Helium, Hydrogen, and Neon.

Once calibration was complete, we installed the spectrometer on a mount and tripod. B. Boe, the lead operator for the spectroscopic observations at Mamalluca, used the slit mirror to align the optical lens on the corona. He also took all measurements during and after the eclipse.

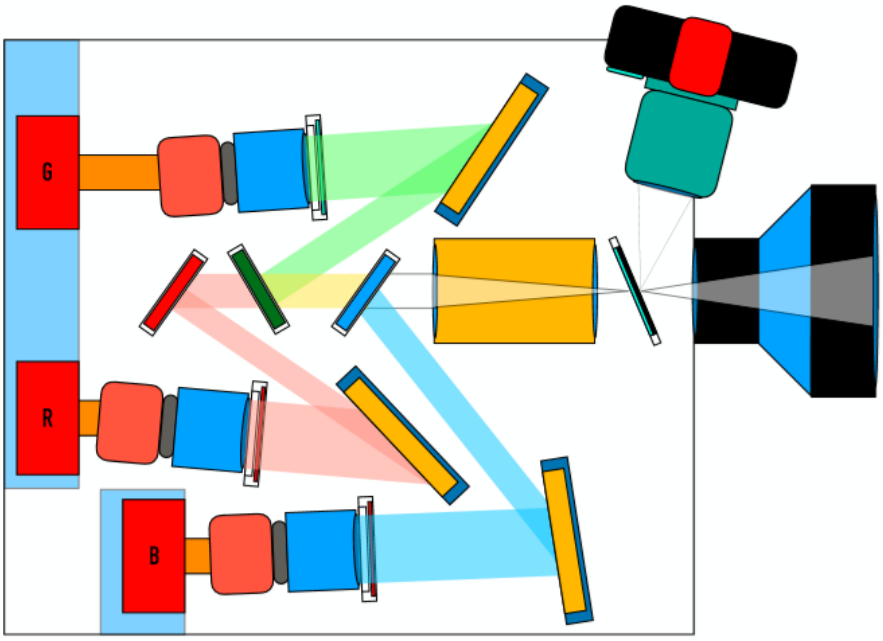

Figure 3.7: Layout of the triple-channel 3-PaMIS spectrometer. Image credit: B. Yamashiro.

Spectroscopic data from the eclipse were taken starting a few minutes leading to- and through- totality. Images were captured with various different exposure times in the three channels.

The fourth camera was used to show the slit position on the corona.

For image calibration, darks were taken immediately after the eclipse with matching exposure times. Flat fields were taken the night before using white paper and a cell phone flashlight. Calibration images were also taken the night before using argon, water, hydrogen, helium, and neon spectral lamps. These calibration images are used to prepare images for data analysis.

4 DATA

4.1 DATA COLLECTION

A total of 71 images were taken over the course of totality for the 2019 TSE, with varying exposure times listed in the table here:

Channel	**Red**	**Green**	**Blue**
Exposure Time (seconds)	2, 7, 15	1, 5, 12	3, 10, 30

Dark frames, flat frames, and biases are applied to light frames to account for imperfections within the imaging system. MaxIm DL, an astronomical imaging software, was used to calibrate all spectra.

54 dark frames were taken immediately after totality by covering the camera lens on the spectrometer with a lens cap and a black bag to ensure no light exposure in the device. Exposure times for the dark frames matched the exposure times of the light frames. Because the dark frames contain random noise from camera interference, subtracting the darks from the light frames will remove noise from the final images. These darks were subtracted from the flat frames (before flat frames were applied to light frame) and light frames using MaxIm DL.

Flat frames were taken of the flat sky (an area of the blue sky low on the horizon, away from the Sun) the day before totality. Flat frames are taken to account for interference during total illumination (for example dust on the lens). A total of seven flat frames were used during image processing, and all had a 30 second exposure time.

4.2 Data Analysis

After image calibration, one must orient the data using solar north. By comparing processed white light images to the slit camera images (see figure 4.1), one can determine orientation of the Sun by observing features of the corona.

Figure 4.1: Two stills from the slit camera, with solar north pointing down. Left is C2 and right is C3. The black line marks the spectrometer slit, denoting the location of where the data were taken in the corona.

For this project, I observed phases C2 and C3 of the TSE (the phases where the moon starts to completely cover the Sun, and where the total solar eclipse ends), in which we can see a visible diamond ring to obtain information on where the Sun is oriented in the 4th camera. I determined solar north was pointing down within the 4th camera.

Spectra were recorded in all three channels, but the blue channel was very weak compared to the red and green. The spectrum of the Sun is primarily Hydrogen and Helium, which are strongest in the red and green channels, so the fact that the signal in the blue channel is weak may not be surprising.

Figure 4.2: Balmer lines, which appear in the Hydrogen spectrum.

Figure 4.3: Helium emission spectrum.

In addition, flat field images from the blue channel had low counts, which may contribute to additional noise in the final processed images. This is discussed more in section 5 (see figure 5.2).

Hydrogen abundance in the Sun is useful for calibration because hydrogen has strong emission lines ranging from red to blue (although the blue emission can be weak). The coronal spectra shows multiple orders of diffraction, making them difficult to interpret. However, comparing them with Hydrogen calibration spectra, we can attempt to identify some of the Hydrogen lines present in the corona. (See figures 4.3 and 4.4)

Qualitatively, the spectra from different parts of the corona look different, and these differences are discussed in the next section. Future (and more complicated) analysis of the spectra in the different channels could lead to insight about the composition and speed of ions in the corona.

4.3 HYDROGEN

The red channel was used for Hydrogen analysis due to the abundance of Hydrogen in the spectra and the strong, red, H α line (see figure 4.2). To showcase the quantitive data found within the spectra of the Sun, I used MaximDL to select a horizontal line of pixels centered on the most intense parts of the spectrum. A line profile plot is a plot of pixel intensity as a function of horizontal pixel location. The plots associated with the calibrated images are seen to the right. Figure 4.4 was taken the night before totality within the darkroom mentioned in section 3.4. Figure 4.6 was taken during totality, note the black band within the middle is the moon. The line profile plot was taken from the top spectra.

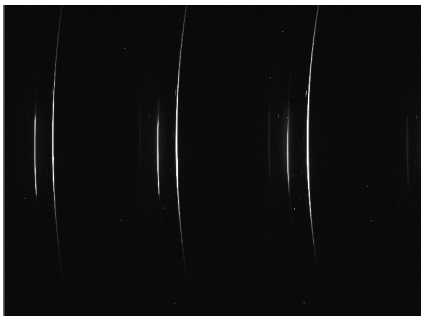

Figure 4.4: Hydrogen calibration in red channel.

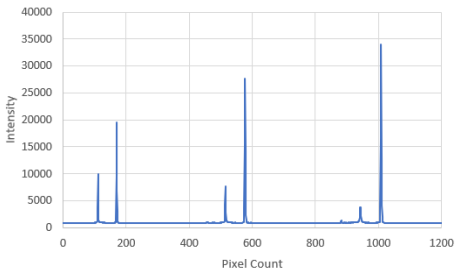

Figure 4.5: Line profile plot of hydrogen calibration in the red channel

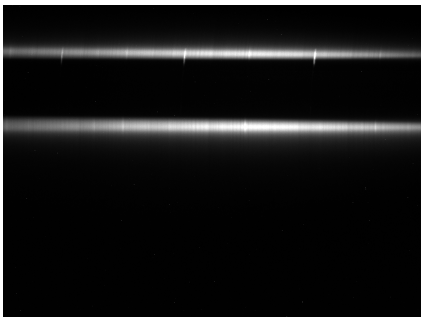

Figure 4.6: Red channel with 2 second exposure during totality (after C2 phase).

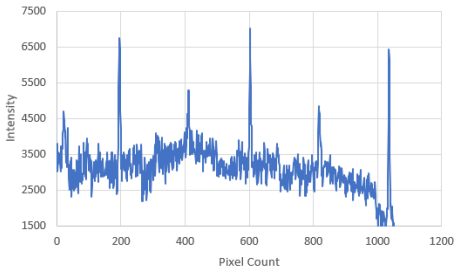

Figure 4.7: Line profile plot of figure 4.6, peaks are correlative with hydrogen spectra.

By comparing the two line profile plots in figures 4.5 and 4.7, three peaks are present $\sim 180, 600, 1000$ in both graphs.

4.4 Helium

The green channel was used for Helium analysis due to its numerous strong spectral lines, and presence of green (see figure 4.3).

The same process used in Hydrogen analysis was applied to the green channel for Helium. MaximDL was used to select a horizontal line of pixels centered around the most intense part of the spectrum. Figure 4.8 was taken utilizing the dark room and a Helium spectral lamp. Figure 4.10 was taken during totality, with the line profile plot of the top spectra in figure 4.11.

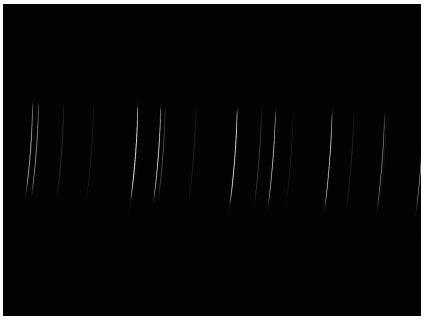

Figure 4.8: Helium calibration in green channel.

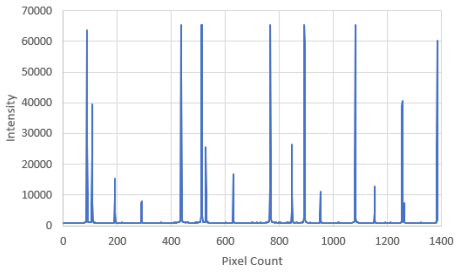

Figure 4.9: Line profile plot of helium calibration in the green channel.

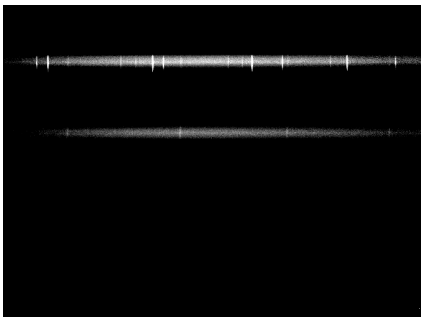

Figure 4.10: Green channel during totality with a 1 second exposure (after C2 phase).

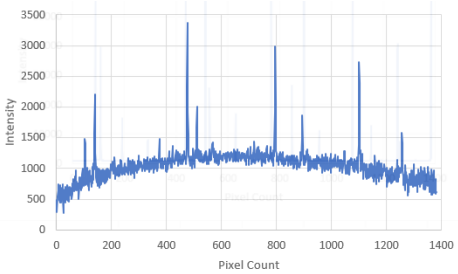

Figure 4.11: Line profile plot of figure 4.10, peaks are correlative with Helium spectra.

5 Conclusion and Future Work

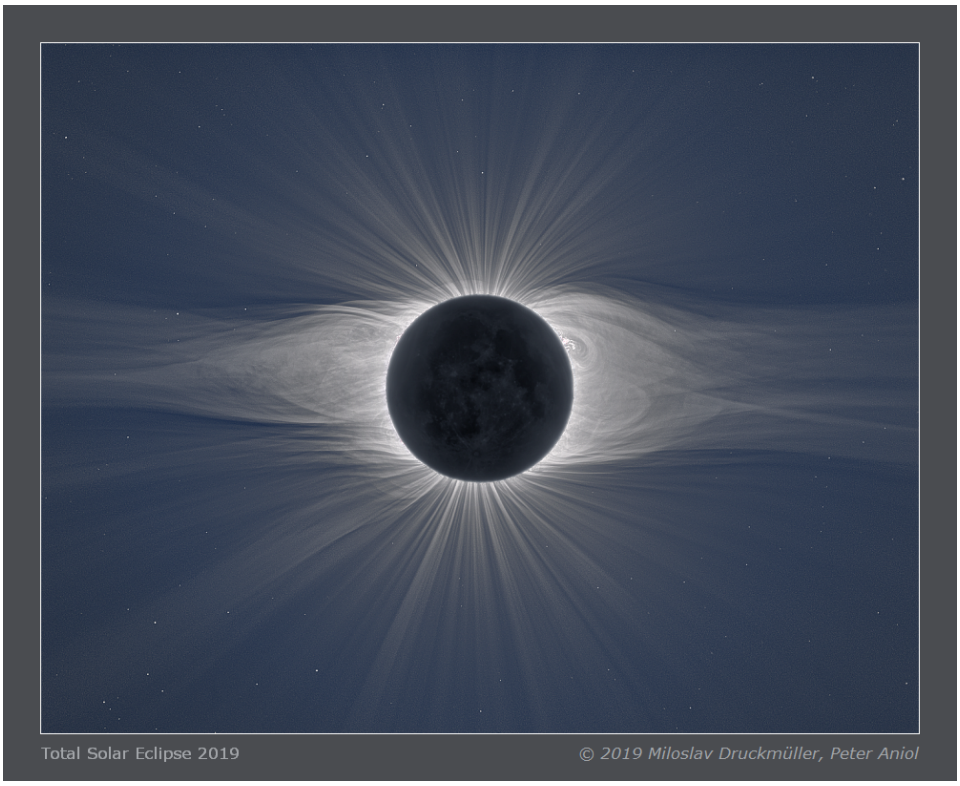

Figure 5.1: White light image of the 2 July 2019 total solar eclipse in Chile. [8]

To further analyze spectra from the eclipse, a few issues must be addressed. Due to the nature of the lenses used, the spectral lines are curved. This curvature must be corrected via alternative methods. After numerous discussions with the team, we believe it is due to the mirrors of the optical setup within the spectrometer. Bryan Yamashiro, Ph.D. candidate at the Institute of Astronomy, recently completed a semester project on how to correct this curvature utilizing python. [10]

As mentioned previously, compared to the red and green channels, the blue channel does not have strong spectral lines, and a very low single to noise radio (see figure 5.2). This may be due to low chip sensitivity to blue light, mis-alignment of the blue channel, or simply faint emission from the Sun in these wavelengths.

The spectrometer design can be improved for future eclipses. The three channel design

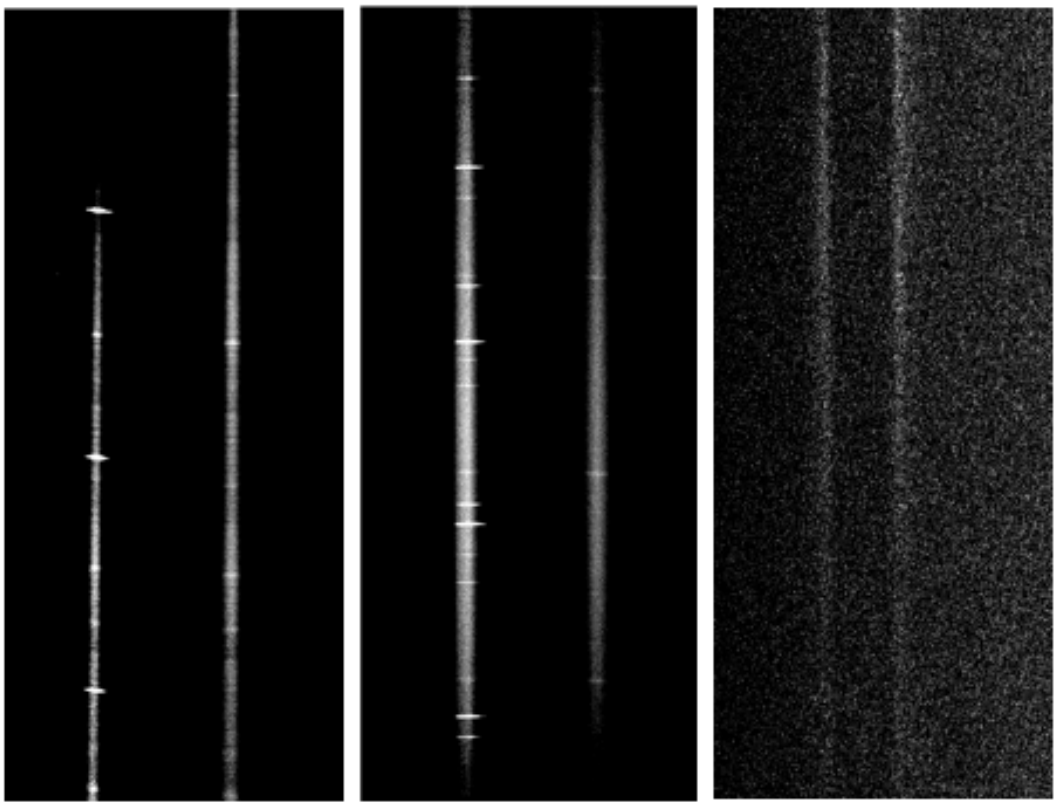

Figure 5.2: The three different channel spectra images taken during totality at Mamalluca. From left to right: Red channel, green channel, blue channel. The black band that appears in the middle is the moon.

is great for transportation and ease of use, but the diachroic mirror used in the design is not a perfect mirror, and allowed for light leaks. This leads to error within the data must be corrected.

The Solar Wind Sherpa expedition to observe the total solar eclipse on July 2, 2019, was a great success. Three teams were spread across Chile and Argentina to observe this event and all three were able to gather data from the solar corona. I got hands-on experience alongside professionals in the field, and I gained valuable knowledge about spectroscopy, the Sun, and how to be part of a large team all working toward the same goal.

REFERENCES

[1] Nasa - solar eclipse. https://eclipse.gsfc.nasa.gov/solar.html. (Accessed on 04/30/2020).

[2] Solar cycle 25 prediction. http://www.cessi.in/solarcycle25prediction/. (Accessed on 02/20/2020).

[3] The solar wind sherpas. https://project.ifa.hawaii.edu/solarwindsherpas/science-news/instruments/. (Accessed on 04/30/2020).

[4] The structure and composition of the sun | astronomy. https://courses.lumenlearning.com/astronomy/chapter/the-structure-and-composition-of-the-sun/. (Accessed on 05/05/2020).

[5] The sun | nasa/goddard. https://www.nasa.gov/mission_pages/sunearth/multimedia/Sunlayers.html. (Accessed on 10/20/2019).

[6] A. Ding. First detection of prominence material embedded within a 2× 106 k cme front streaming away at 100-1500 km s- 1 in the solar corona.

[7] D. D. H. Hathaway. Nasa/marshall solar physics. https://solarscience.msfc.nasa.gov/interior.shtml, October 2015. (Accessed on 10/30/2019).

[8] Miloslav. Baily's beads detail | 2005 total solar eclipse. http://www.zam.fme.vutbr.cz/~druck/Eclipse/Ecl2005d/Ecl2005_2nd_bp448an/0-info.htm. (Accessed on 10/20/2019).

[9] T. Sharp. Atmosphere of the sun: Photosphere, chromosphere & corona. https://www.space.com/17160-sun-atmosphere.html, November 2017. (Accessed on 10/20/2019).

[10] B. Yamashiro, S. Habbal, A. Ding, and M. Nassir. On the Inference of Fe^{+9} Ion Temperature in the Solar Corona from the 2019 July 2 Total Solar Eclipse. In *American Astro-*

nomical Society Meeting Abstracts, American Astronomical Society Meeting Abstracts, page 210.02, Jan. 2020.